[Regular Paper]

Isomerization of *n*-Hexadecane over Pt–WO_3 Catalysts Supported on TiO_2–SiO_2 Mixed Oxides Synthesized by Glycothermal Method

Saburo HOSOKAWA, Shota KAMISHIMA, Koichi KUBO, Hiroyoshi KANAI, Kenji WADA, and Masashi INOUE*

Dept. of Energy and Hydrocarbon Chemistry, Graduate School of Engineering, Kyoto University, Katsura, Nishikyo-ku, Kyoto 615-8510, JAPAN

(Received May 31, 2011)

The isomerization of *n*-hexadecane over Pt–WO_3 catalysts supported on TiO_2–SiO_2 synthesized by glycothermal reaction with various Si/Ti molar ratios was examined. The catalyst performance depended on Si/Ti molar ratio and WO_3 loading. The characterization of the catalysts by XRD, XAFS, UV-vis and so on revealed that with increasing the WO_3 loading, the structure of surface W species changed from monomeric species to polytungstate species, which is considered to significantly affect the isomerization selectivity of the catalysts.

Keywords

n-Hexadecane, Isomerizaiton, Titania–silica, Tungusten oxide, Glycothermal method

1. Introduction

Fischer-Tropsch synthesis is well known as a method for preparing liquid fuels from syngas that can be made from carbon resources such as natural gas, coal, and biomass. The fuel obtained by this reaction does not contain nitrogen, sulfur and aromatic compounds, and is expected as a future fuel that takes the place of petroleum[1]. Since this liquid fuel predominantly consists of *n*-paraffins, it has a low octane number for the use as gasoline[2),3)]. Furthermore, *n*-paraffins can not be used for diesel oil and lube oil in the cold latitudes because of low fluidity at low temperatures. For these reasons, *n*-paraffins are required to be isomerized[2),3)].

Bifunctional catalysts such as Pt–WO_3/ZrO_2[4),5)], Pt–SO_4^{2-}/ZrO_2[6),7)] and Pt/zeolite[8),9)] are used for isomerization of *n*-paraffins. According to the classical isomerization mechanism[10)], paraffins are dehydrogenated on the metal sites, and the formed olefins are protonated on the acid sites yielding the corresponding alkylcarbenium ions. These carbenium ions undergo skeletal rearrangement or β-scission followed by deprotonation and hydrogenation over the metal sites to yield the corresponding paraffins.

We have been exploring the synthesis of inorganic materials by glycothermal reactions in 1,4-butanediol at elevated temperatures (200-300 ℃) under the autogenous pressure of the organics[11),12)]. In the previous work, we reported that Si-modified TiO_2 with the anatase structure having high thermal stabilities was prepared by glycothermal reaction[13)].

In the present paper, isomerizations of *n*-hexadecane on Pt–WO_3/TiO_2–SiO_2 catalysts were examined for the synthesis of diesel oil. The effects of WO_3 loading and the reaction conditions as well as the Si/Ti molar ratio of the TiO_2–SiO_2 support synthesized by the glycothermal method upon the yield of branched C_{16} hydrocarbons (*i*-hexadecanes) were examined.

2. Experimental

2. 1. Synthesis of TiO_2 and TiO_2–SiO_2 Supports by the Glycothermal Method

Desired amounts of titanium isopropoxide and tetraethyl orthosilicate were added to 1,4-butanediol and this mixture was placed in a 960-mL autoclave equipped with a Liebig condenser of stainless-steel tubing. After the atmosphere inside the autoclave was replaced with nitrogen, the assembly was heated to 300 ℃ and kept at that temperature for 2 h. The outlet valve of the autoclave was, then, slightly opened while keeping the autoclave temperature at 300 ℃, and the organic vapor was removed from the autoclave by flash evaporation. After cooling, bulky solid products were directly obtained as xerogels. The products were calcined in air at 600 ℃ for 1 h to eliminate the surface organic moieties. The thus-obtained products are designated as XG(x), where x is the Si/Ti charged ratio.

The glycothermal product was also recovered by

This paper was presented at the 13th Japanese-Korea Symposium on Catalysis, Jeju, Korea, May 23-25, 2011.

* To whom correspondence should be addressed.
* E-mail: inoue@scl.kyoto-u.ac.jp

Table 1 Performance of 0.6 wt% Pt–15 wt% WO_3/XG(x) Catalysts for Isomerization of n-C_{16}[a)]

x = Si/Ti	0	0.1	0.2	0.3
n-C_{16} conversion [%]	71.2	70.1	65.8	52.3
i-C_{16} selectivity	21.4	24.6	40.8	22.6
Monobranched i-C_{16}	7.1	8.0	14.6	7.2
Dibranched i-C_{16}	8.5	9.9	15.8	9.1
Tribranched i-C_{16}	5.8	6.7	10.4	6.3
i-C_{16} yield	15.2	17.2	26.8	11.9
BET S.A. [m^2/g]	76	121	130	156

a) Reaction conditions: Catalyst, 2 g; n-C_{16}, 50 mL; Reaction temperature, 300 ℃; Reaction time, 2 h; H_2 3.0 MPa (r.t.).

another method: After the glycothermal reaction, the assembly was cooled and the product was washed with acetone repeatedly by vigorous mixing and centrifuging. The product was dried in an 80 ℃ oven, and then calcined in air at 600 ℃ for 1 h. The thus-obtained products are designated as GT(x), where x is the Si/Ti charged ratio.

2. 2. Tungsten Loading on the XG(x) and GT(x) Supports

A desired amount of ammonium paratungstate ($5(NH_4)_2O \cdot 12WO_3 \cdot 5H_2O$) was dissolved in100 mL of water at 60 ℃ and the catalyst support was added to this solution. Excess water was removed on a rotary evaporator and the catalyst was dried in an 80 ℃ oven.

2. 3. Platinum Loading on WO_3/XG(x) and WO_3/GT(x)

The powder after supporting tungsten was added to an aqueous solution containing a desired amount of H_2PtCl_6, and the slurry was dried on an 80 ℃ water bath, followed by calcination in air at 600 ℃ for 1 h.

2. 4. Isomerization of n-Hexadecane over Pt–WO_3/XG(x) and Pt–WO_3/GT(x) Catalysts

The catalyst (2.0 g) was pretreated with hydrogen at 300 ℃ for 1 h and then added to 50 mL of n-hexadecane in a 300-mL autoclave. After the atmosphere inside the autoclave was replaced with nitrogen, hydrogen was introduced to the autoclave until the pressure inside the autoclave reached 3.0 MPa. This assembly was heated to 300 ℃ and kept at that temperature for 2-8 h. After cooling, the resulting solution was analyzed by gas chromatography (Shimadzu GC-14A).

2. 5. Characterization of the Catalysts

Powder X-ray diffraction (XRD) pattern was recorded on a diffractomater, Shimadzu XD-D1, using Cu Kα radiation and a carbon-monochromator. Specific surface area of the sample was calculated by the BET single-point method on the basis of the nitrogen uptake measured at 77 K using a Micromeritics Flowsorb II 2300 sorptionmeter. The UV-vis absorption spectra of the catalysts were recorded on a JASCO V-650DS spectrophotometer. The W L_1 and L_3-edge X-ray absorption fine structure (XAFS) spectra were recorded in air at room temperature using the facility of the BL16B2 beam line at SPring-8 of the Japan Synchrotron Radiation Research Institute.

3. Results and Discussion

3. 1. Catalyst Activity

The effects of the Si/Ti ratio of the XG(x) support on the isomerization reaction over Pt–WO_3 catalysts supported on TiO_2 or TiO_2–SiO_2 are shown in **Table 1**. The conversion of n-hexadecane increased with the increase in the titanium concentration in the support. This result is opposite to that expected from BET surface area of the catalyst. However, hydrocracking predominantly occurred for the catalyst supported on XG(0), and the highest selectivity and yield of i-hexadecanes were obtained by the catalyst with Si/Ti = 0.2.

The effect of WO_3 loadings on the isomerization performance of 0.6 wt% Pt–WO_3/XG(0.2) catalysts with various WO_3 loadings are shown in **Table 2**. The conversion of n-hexadecane increased with the increase in the WO_3 loading and leveled off at higher WO_3 loadings. The selectivity for i-hexadecanes decreased with the increase in WO_3 loading, and the highest yield of i-hexadecanes was attained by 15 wt% WO_3 loading.

Table 3 shows the results of isomerization reaction over 0.6 wt% Pt–WO_3/GT(0.2) catalysts. With increasing the WO_3 loading, the n-hexadecane conversion increased while the i-hexadecane selectivity decreased. This tendency is the same as that observed for 0.6 wt% Pt–WO_3/XG(0.2) catalysts (**Table 2**). When the performances of the catalysts with the optimum composition were compared, the yield of i-hexadecanes obtained on the GT(0.2)-supported catalyst was slightly higher than that on the XG(0.2)-supported catalyst, and the optimum WO_3 loading for the GT catalyst was lower than that for the XG catalyst.

We have previously reported that the pore structure of the glycothermal products was drastically altered by the removal of the glycol at the reaction temperature after the glycothermal reaction (XG method), and the silica-modified TiO_2 having a large macropore volume was obtained by the XG method, which had higher

Table 2 Performance of 0.6 wt% Pt–WO_3/XG(0.2) Catalysts for Isomerization of *n*-C_{16}[a)]

WO_3 loading [wt%]	5	10	15	20	23.1	28.7
n-C_{16} conversion [%]	3.2	18.7 (64.7)[b)]	65.8	65.8	68.2	66.6
i-C_{16} selectivity	98.7	96.1 (80.5)	40.8	20.5	24.4	29.6
Monobranched *i*-C_{16}	80.6	61.8 (34.1)	14.6	6.5	6.5	9.4
Dibranched *i*-C_{16}	18.1	26.4 (30.2)	15.8	6.8	9.1	11.8
Tribranched *i*-C_{16}	0.0	7.9 (16.2)	10.4	7.2	8.8	8.4
i-C_{16} yield	3.3	18.0 (52.1)	26.8	13.5	16.6	19.8

a) Reaction conditions: Catalyst, 2 g; *n*-C_{16}, 50 mL; Reaction temperature, 300 ℃; Reaction time, 2 h; H_2 3.0 MPa (r.t.).
b) Reaction time; 8 h.

Table 3 Performance of 0.6 wt% Pt–WO_3/GT(0.2) Catalysts for Isomerization of *n*-C_{16}[a)]

WO_3 loading [wt%]	5	10	15	20	25	30
n-C_{16} conversion [%]	5.5	38.5 (77.1)[b)]	69.7	66.0	66.1	73.1
i-C_{16} selectivity	90.8	95.3 (76.1)	29.2	22.4	22.4	20.8
Monobranched *i*-C_{16}	76.8	51.5 (27.8)	9.8	7.4	7.2	6.5
Dibranched *i*-C_{16}	12.9	33.2 (30.1)	11.7	9.1	9.2	8.5
Tribranched *i*-C_{16}	1.1	10.6 (18.2)	7.7	5.9	6.0	5.8
i-C_{16} yield	5.0	36.7 (58.7)	20.4	14.8	14.8	15.2

a) Reaction conditions: Catalyst, 2 g; *n*-C_{16}, 50 mL; Reaction temperature, 300 ℃; Reaction time, 2 h; H_2 3.0 MPa (r.t.).
b) Reaction time; 8 h.

photocatalytic activity than the product obtained by the ordinary GT method[14]. In the present case, the dispersion of W species affects the catalytic activity, and the formation of WO_x cluster was important for the isomerization, as discussed later. The particles of the XG support are easily dispersed in water because the sample does not suffer from coagulation that usually takes place during the drying stages of the powder preparation procedures. Therefore, highly dispersed W species are easily formed on the XG support. On the other hand, diffusion of bulky polytungstate species in the pore system of the GT support is required during the impregnation process, which reduces the effective surface area of the support, and WO_x clusters are easily formed on the GT support at a low WO_3 loading.

The results of isomerization reaction with prolonged reaction time are also shown in **Tables 2** and **3**. The 0.6 wt% Pt–10 wt% WO_3 catalysts supported on XG(0.2) and GT(0.2) were used. By prolonging the reaction time for 8 h, the conversion of *n*-hexadecane increased with maintaining high *i*-hexadecane selectivity. The 0.6 wt% Pt–10 wt% WO_3/GT(0.2) catalyst showed higher catalytic activity than 0.6 wt% Pt–10 wt% WO_3/XG(0.2) and afforded *i*-hexadecanes in a yield of 58.7 %.

3. 2. State of WO_x on TiO_2–SiO_2

From the XRD patterns of the 0.6 wt% Pt–WO_3/XG(0.2) catalysts, the peaks due to anatase TiO_2 and PtO were observed in all the samples (**Fig. 1**). The peak intensity due to PtO decreased with the increase in the WO_3 loading, suggesting that the proportion of highly dispersed Pt species increased with the increase in WO_3 loading. Keogh *et al*. have reported the effect of the Pt loading on the performance of sulfated ZrO_2 catalysts for the hydroisomerization of *n*-hexadecane[7]. They reported that the conversion of *n*-hexadecane drastically increased with the increase in the Pt loading up to 0.6 wt%, while further increase in the Pt loading caused a slight decrease in the conversion. On the other hand, the selectivity was reported to be a function of conversion and not to change with the Pt loading when compared at a constant level of conversion[7]. In the present work, the Pt loading was fixed at 0.6 wt%, since various factors such as Si content, WO_3 loading and preparation method of TiO_2 must be controlled.

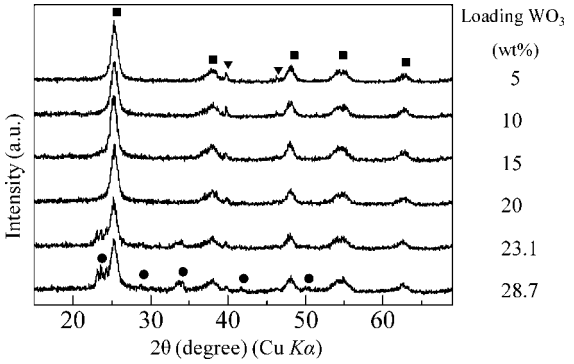

●, monoclinic WO_3; ■, anatase TiO_2; ▼, PtO.

Fig. 1 XRD Patterns of the 0.6 wt% Pt–WO_3/XG(0.2) Catalysts

The catalysts with 23.1 and 28.7 wt% WO_3 loadings showed the XRD peaks due to monoclinic WO_3. However, WO_x species were not observed in the catalysts with the WO_3 loadings less than 20 wt%. This result indicates that crystallized WO_3 species on catalysts does not participate in the isomerization, thus the

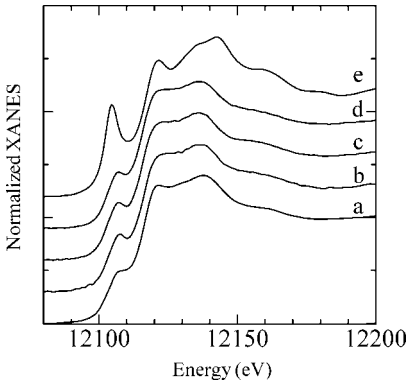

a, WO_3; b, 5 wt% WO_3/XG(0.2); c, 10 wt% WO_3/XG(0.2); d, 20 wt% WO_3/XG(0.2); e, Na_2WO_4.

Fig. 2 W L_1-edge XANES Spectra of WO_3/XG(0.2) Catalysts and Standard Samples

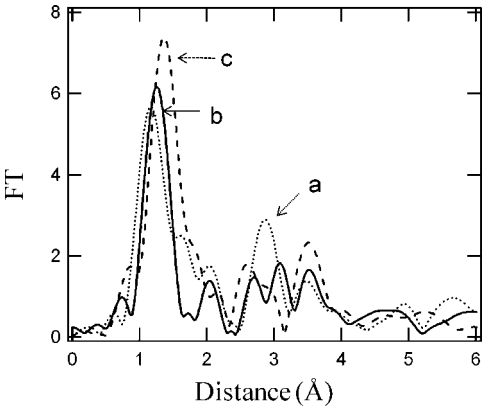

a, 5 wt%; b, 20 wt%; c, WO_3.

Fig. 3 Fourier Transforms of W L_3-edge EXAFS Oscillations of WO_3/XG(0.2)

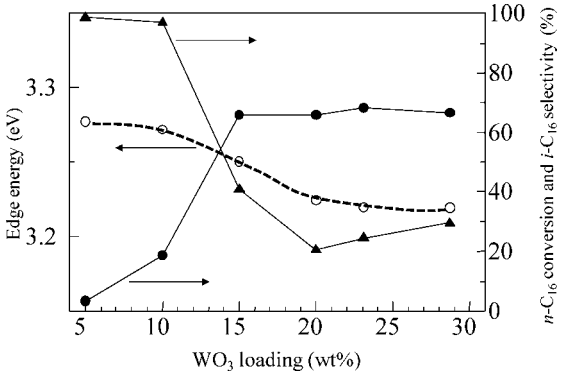

Fig. 4 *n*-Hexadecane Conversion (●) and *i*-Hexadecane Selectivity (▲) of the 0.6 wt% Pt–WO_3/XG(0.2) Catalysts and Edge Energy Calculated from UV-vis Spectra of WO_3/XG(0.2) Calcined at 600 ℃ (○) as Plotted against the WO_3 Loading

conversion of *n*-hexadecane almost being unchanged at higher WO_3 loadings.

Figure 2 shows W L_1-edge X-ray absorption near edge structure (XANES) spectra of the WO_3/XG(0.2) samples with various WO_3 loadings and two standard samples. The pre-edge peak was clearly observed for $NaWO_4$ in which W atoms have a tetrahedral coordination structure, while the intensity of the pre-edge peak was much weaker for WO_3 where W atoms have a distorted octahedral structure. The pre-edge peak is attributed to forbidden electron transitions from 2s orbital to 5d orbitals. A less symmetric W structure (distortion from O_h symmetry) provides an intense pre-edge peak because this transition is allowed by mixing the p orbitals with empty d orbitals of tungsten[15]. The features of the spectra of all the samples resembled that of WO_3. Therefore, WO_x species having a WO_3-like structure was formed on TiO_2–SiO_2. However, the intensity of the pre-edge peak in the WO_3/XG(0.2) samples was higher than that observed for the WO_3 standard, indicating that the average coordination structure of the WO_x species on TiO_2–SiO_2 was more distorted as compared with WO_3.

Figure 3 shows the Fourier transform (FT) spectra of the W L_3-edge extended X-ray absorption fine structure (EXAFS) oscillations. The spectra of the WO_3/XG(0.2) samples were different from that of the WO_3 standard in the first and second shells at 0.5-4.0 Å (1 Å = 10^{-10} m). The average length of the W–O bond as estimated from the first shell decreased with decreasing the WO_3 loading, indicating that the W–O bond in the WO_x species in the catalysts with low WO_3 loadings has double-bond nature. The shape of the second shell peak of the catalyst was different from that of the WO_3 reference and a peak at 2.9 Å was clearly observed for 5 wt% WO_3/XG(0.2). As Hilbrig *et al.* reported[16], this peak seems to correspond to W–Ti distance. These results indicates that the double-bond nature of the W–O bond in the WO_x species in the catalysts with low WO_3 loadings is caused by strong interaction of WO_x species with the support.

The edge energies calculated from UV-vis spectra of the WO_3/XG(0.2) samples calcined at 600 ℃ are plotted against the WO_3 loading (**Fig. 4**). The edge energy was observed at ~3.274 eV for 5-10 wt% WO_3 samples, and decreased to about 3.218 eV by the increase in the WO_3 loading to 20 wt%, while further increase in the WO_3 loading did not decrease the edge energy. Barton *et al.* reported that the domain size of W species can be evaluated from the edge energy calculated from the UV-vis spectrum; the catalyst having a high edge energy had highly dispersed W species on the support[17].

The present results suggest that the catalyst with $<$10 wt% WO_3 loadings has highly dispersed WO_x species on the support, while crystalline WO_3 was formed for the catalyst with $>$23 wt% WO_3 loadings, which was verified by the XRD patterns. In the intermediate range from 10 to 20 wt% WO_3, polytungstate species[17] seem to be formed and the XAFS analysis indicates that

these polytungstate species had distorted octahedral W structures. In **Fig. 4**, the *n*-hexadecane conversion and the *i*-hexadecane selectivity in isomerization reaction over 0.6 wt% Pt–WO_3/XG(0.2) catalysts are also plotted. The behavior for edge energy resembled that of the *i*-hexadecane selectivity, suggesting that the aggregation state of WO_x species controls the performance of the catalyst for isomerization of *n*-hexadecane.

4. Conclusions

The isomerization of *n*-hexadecane over the Pt–WO_3 catalysts supported on TiO_2–SiO_2 mixed oxides was examined. In the XG(*x*) supports with various Si/Ti molar ratios synthesized by the glycothermal method, the support with Si/Ti＝0.2 (XG(0.2)) showed the highest performance. The XAFS and UV-vis spectra suggested the structure of WO_x species changed from monomeric highly dispersed WO_x to polytungstate species and to crystalline WO_3 by increasing the WO_x loading. The highly dispersed WO_x species had low activity and crystalline WO_3 species hardly contributed to the reaction. The polytungstate species has an important role for the isomerization.

The *n*-hexadecane conversion over the catalysts supported on GT(0.2) was slightly higher than that observed for the XG(0.2)-supported catalyst, and 58.7 % yield of *i*-hexadecanes was attained by prolonging the reaction over 0.6 wt% Pt–10 wt% WO_3/GT(0.2) catalyst.

Acknowledgments

The authors thank Dr. Tsunenori Watanabe and Dr. Hiroshi Deguchi of The Kansai Electric Power Co., Inc. for the measurement of XAFS spectra.

References

1) Schulz, H., *Appl. Catal. A: General*, **186**, 3 (1999).
2) Deldari, H., *Appl. Catal. A: General*, **293**, 1 (2005).
3) Zhou, Z., Zhang, Y., Tierney, J. W., Wender, I., *Fuel Process. Technol.*, **83**, 67 (2003).
4) Busto, M., Grau, J. M., Vera, C. R., *Appl. Catal. A: General*, **387**, 35 (2010).
5) Martínez, A., Prieto, G., Arribas, M. A., Concepción, P., Sánchez-Royo, J. F., *J. Catal.*, **248**, 288 (2007).
6) Keogh, R. A., Srinivasan, R., Sparks, D. E., Khorfan, S., Davis, B. H., *Fuel*, **78**, 721 (1999).
7) Keogh, R. A., Srinivasan, R., Davis, B. H., *Appl. Catal. A: General*, **140**, 47 (1996).
8) Mochizuki, T., Toba, M., Abe, Y., Yoshimura, Y., *J. Jpn. Petrol. Inst.*, **52**, (3), 143 (2009).
9) Soualah, A., Lemberton, J. L., Pinard, L., Chater, M., Magnoux, P., Moljord, K., *Appl. Catal. A: General*, **336**, 23 (2008).
10) Weisz, P. B., *Adv. Catal.*, **13**, 137 (1962).
11) Inoue, M., "Chemical processing of ceramics," 2nd ed., eds. by Lee, B., Komarneni, S., Taylor & Francis, Boca Raton, FL (2005), Chap. 2, p. 22-63.
12) Iwamoto, S., Inoue, M., *J. Jpn. Petrol. Inst.*, **51**, (3), 143 (2008).
13) Iwamoto, Sh., Iwamoto, Se., Inoue, M., Yoshida, H., Tanaka, T., Kagawa, K., *Chem. Mater.*, **17**, 650 (2005).
14) Iwamoto, S., Saito, K., Inoue, M., Kagawa, K., *Nano Lett.*, **1**, 417 (2001).
15) Yamazoe, S., Hitomi, Y., Shishido, T., Tanaka, T., *J. Phys. Chem. C.*, **112**, 6869 (2008).
16) Hilbrig, F., Göbel, H. E., Knözinger, H., Schmelz, H., Lengeler, B., *J. Phys. Chem.*, **95**, 6973 (1991).
17) Barton, D. G., Shtein, M., Wilson, R. D., Soled, S. L., Iglesia, E., *J. Phys. Chem. B*, **103**, 630 (1999).

……

要　　旨

グリコサーマル合成した TiO_2–SiO_2 複合酸化物上に担持した Pt–WO_3 触媒による *n*-ヘキサデカンの異性化

細川　三郎，上島　祥太，久保　浩一，金井　宏俶，和田　健司，井上　正志

京都大学大学院工学研究科物質エネルギー化学専攻，615-8510 京都市西京区京都大学桂

グリコサーマル合成した TiO_2–SiO_2 複合酸化物上に担持した Pt–WO_3 触媒による *n*-ヘキサデカンの異性化を検討した。触媒活性は Ti/Si モル比や WO_3 担持量に依存していることが認められた。その結果，グリコサーマル合成した TiO_2–SiO_2（Ti/Si＝0.2）に担持した 0.6 wt% Pt–10 wt% WO_3 触媒が最も高い活性を示し，58.7 % の *i*-ヘキサデカン収率が得られた。また，XRD 測定，XAFS 測定および UV-vis 測定により触媒の構造解析を行い，WO_3 担持量の増加とともに，表面 W 種は単核種から複核種，さらに WO_3 に変化することを明らかにした。この W 種の構造変化が *n*-ヘキサデカンの異性化に対して大きく影響を及ぼしていることが認められた。

……